Journal of Ambient Intelligence and Humanized Computing (2021) 12:1069–1080
https://doi.org/10.1007/s12652-020-02142-4

ORIGINAL RESEARCH

Comparative study of Pareto optimal multi objective cuckoo search algorithm and multi objective particle swarm optimization for power loss minimization incorporating UPFC

Nartu Tejeswara Rao[1] · Matta Mani Sankar[2] · Surapu Prasada Rao[1] · Boddepalli Srinivasa Rao[1]

Received: 11 August 2019 / Accepted: 22 May 2020 / Published online: 28 May 2020

Abstract
The Flexible AC Transmission System (FACTS) devices are being commissioned in electrical power systems across the globe owing to the vast array of benefits they offer. The optimal performance of the FACTS devices can be harnessed only if they are installed at a strategic location. In this paper, the authors suggest the merit of multiobjective cuckoo search (MOCS) algorithm in mitigation of transmission losses by strategically installing unified power flower controller (UPFC) at an optimal location. Active power loss and reactive power loss reduction is the multiobjective optimization considered for the study. The Pareto-optimal technique is employed to extract the Pareto-optimal solution for the multiobjective problem considered. The Fuzzy logic method is utilized to yield the best-compromise solution from the pool of Pareto-optimal solution. The proposed approach is tested on a standard IEEE 30 bus test system. Furthermore, the efficacy of the MOCS algorithm is demonstrated by comparing the results with that of multiobjective particle swarm optimization (MOPSO).

Keywords Optimal location · Pareto-optimal technique · Multiobjective cuckoo search algorithm · Multiobjective particle swarm optimization · Unified power flow controller · FACTS

1 Introduction

To keep pace with the ever increasing demand for electrical energy, it has become inevitable for the utilities to increase the generation by adding new generating sources to the existing grid but on the flip-side addition of new generators to the grid involves high capital cost and environmental concerns. Efficient utilization of the existing transmission infrastructure by reducing line losses is an attractive alternative to relieve the grid from the burden of increasing energy demand. Line losses can be reduced by placing FACTS devices (Hingorani Gyugyi 2000) at appropriate locations in the system. Fortunately, the advent of FACTS coincided with deregulation of the electric power sector and many new opportunities unfolded for enhancing the capacity of the existing electrical network (Galiana FD et al. 1996; Mani and Seksena 2017; Nartu et al. 2019). Because of the capital cost involved with the fitting of FACTS devices, it is paramount to trace the optimal location at which the maximum benefits of the installed device can be yielded without violating the system constraints.

UPFC is a versatile member of the FACTS devices family. Its major advantage lies in its potential to simultaneously control active and reactive power. To realize the full capacity of UPFC, it is unequivocally vital to position it at an optimal location. Copious optimization techniques have been proposed for finding the appropriate location to install UPFC for achieving different objectives. The concept of system loading sensitivity is suggested in (Singh and Erlich 2005) to optimally place UPFC in the system. In (Venkatesh and Gooi 2006) the optimal location of UPFC is traced by fuzzy evolutionary programming. In (Shaheen et al. 2008) genetic algorithm (GA) and Particle swarm optimization (PSO) techniques were proposed to screen the optimal position for installation of UPFC. In (Taher and Amooshahi 2012) an approach utilizing a hybrid immune algorithm (HIA) for optimal UPFC placement is developed to achieve optimal

✉ Matta Mani Sankar
che.shankar@gmail.com

[1] Department of Electrical and Electronics Engineering, Aditya Institute of Technology and Management, Tekkali, India

[2] Department of Electrical Engineering, BIT Sindri, Dhanbad, India

power flow. To determine the optimal position of UPFC a gravitational search algorithm (GSA) technique is introduced in (Sarker et al. 2013). The superiority of the hybrid chemical reaction algorithm (HCRO) over its peers PSO and GA in tracing the best position of UPFC is established in (Dutta et al. 2015). A power loss sensitivity index (PLSI) is used in (Shrawane Kapse et al. 2018) to find the optimal location of UPFC. Moth flame optimization (MFO) in its natural form as well as in hybrid form called JAYA blended MFO (JMFO) is applied for finding the optimal location of FACTS devices in (Dash et al. 2019). Although the algorithms used are most recent ones, only single objective is considered in this study. To enhance the dynamic stability of the power system in a recent study reported in (Vijay and Ramaiah 2019) UPFC is optimally located by using modified slap swarm algorithm.

The existing studies on power loss minimization by optimally locating FACTS device are inclined mostly towards single objective optimization. Multiobjective optimization catering to the simultaneous reduction of active and reactive power loss reduction is seldom explored in the available literature. In this paper, a novel attempt is made by the authors by choosing active and reactive power loss reduction as a multiobjective optimization problem. Multiobjective cuckoo search algorithm (MOCS) presented in (Yang and Deb 2011) as an upgrade to the standard CS algorithm (Yang and Deb 2010, 2011) is incorporated for this purpose. The results obtained are compared with that of MOPSO, to the best knowledge of the authors of this article; no such comparison has been reported in the literature so far. The results indicate the superiority of the MOCS algorithm over MOPSO in solving multiobjective optimization problems. In addition to MOPSO, multiobjective firefly algorithm (MOFA) is also implemented to solve the multiobjective optimization problem and compared with MOCS.

The rest portion of this paper is sectioned as follows. Section 2 is about UPFC and its modeling equations. The multiobjective optimization algorithms employed are discussed in Sect. 3. The multiobjective function and the limiting constraints are discussed in Sect. 4. Section 5 deals with the Pareto-optimal method and fuzzy logic method. The numerical results generated are illustrated in Sect. 6. Section 7 outlines the conclusion of the article.

2 Unified power flow controller

UPFC is a multifaceted device under FACTS family which exhibits the capabilities of series compensation, voltage regulation and phase shifting (Gyugyi et al. 1995; Mathur and Varma 2002). The basic model of UPFC is depicted in Fig. 1. It comprises of two voltage source converters (VSC), one interfaced in series with the line and the other connected

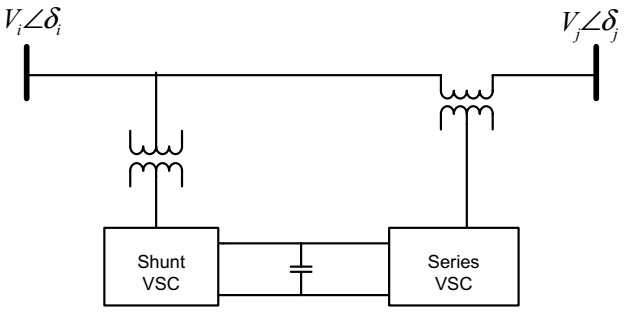

Fig. 1 Basic model of UPFC

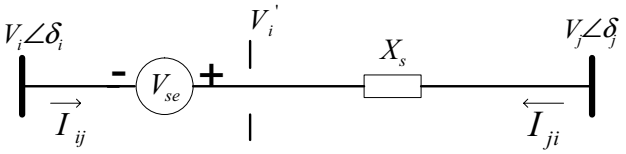

Fig. 2 Series connected VSC model

in shunt with the line through two different interface transformers. A common capacitor bank provides the necessary dc voltage for the converters. The series-connected VSC injects an ac voltage of desired magnitude and phase angle. As a consequence, the series-connected converter trades both active and reactive power with the line. The shunted connected VSC affords the real power demand of the series-connected VSC.

2.1 Steady-state modeling of UPFC

UPFC, as mentioned above, has two converters. The UPFC model used in this study is described below. This model is considered to study the influence of UPFC on the power system under steady-state condition.

2.2 Series connected VSC model

The series VSC can be modeled as a controllable series voltage source V_{se} connected in-between bus-i and bus-j in series with a line of reactance X_s (Noroozian et al. 1997; Mithu 2013). Figure 2 shows the series-connected voltage source converter model and the effect of V_{se} on the system response is

$$V_i' = V_{\text{se}} + V_i \tag{1}$$

Here, V_{se} is controllable in both magnitude and phase

$$V_{se} = rV_i e^{j\gamma} \tag{2}$$

where

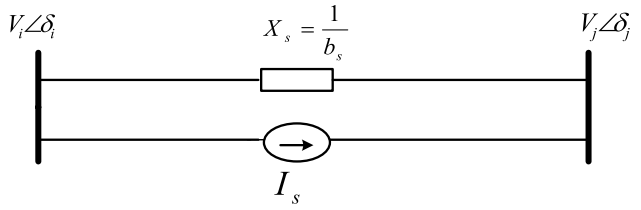

Fig. 3 Injection model of series-connected VSC

$$0 \le r \le r_{\max} \text{ and } 0 \le \gamma \le 360^\circ \tag{3}$$

The injection model as shown in Fig. 3 can be obtained by replacing the voltage source V_{se} with a current source $I_s = -jb_sV_{se}$ in parallel with the line (Noroozian and Andersson 1993)

$$\text{where } b_s = \frac{1}{X_s} \tag{4}$$

The injecting powers S_{is} and S_{js}.corresponding to I_s are given by

$$S_{is} = V_i\left(-I_s\right)^* \tag{5}$$

$$S_{js} = V_j\left(I_s\right)^* \tag{6}$$

Substituting I_s in Eq. (5) and (6),

$$\begin{aligned} S_{is} &= V_i\left(jb_s\left(rV_ie^{j\gamma}\right)\right)^* = P_{is} + jQ_{is} \\ &= -b_srV_i^2\sin\gamma - jb_srV_i^2\cos\gamma \end{aligned} \tag{7}$$

$$\begin{aligned} S_{js} &= V_j\left(-jb_s\left(rV_ie^{j\gamma}\right)\right)^* = P_{js} + jQ_{js} \\ &= b_srV_iV_j\sin\left(\delta_{ij}+\gamma\right) + jb_srV_iV_j\cos\left(\delta_{ij}+\gamma\right) \end{aligned} \tag{8}$$

where δ_{ij} represents the phase shift between bus-i and bus-j respectively.

2.3 Shunt-connected VSC model

The shunt converter in UPFC maintains constant voltage profile within tolerable limits. It also supplies active power which is fed into the system through a voltage source connected in series. If we neglect the losses then

$$P_{\text{conv1}} = P_{\text{conv2}} \tag{9}$$

The apparent power supplied by the series voltage source converter is

$$\begin{aligned} S_{\text{conv2}} &= V_sI_{ij}^* = P_{\text{conv2}} + jQ_{\text{conv2}} \\ &= rV_ie^{j\gamma}\left(\frac{V_i' - V_j}{jX_s}\right)^* \end{aligned} \tag{10}$$

After simplification,

$$P_{\text{conv2}} = b_srV_iV_j\sin\left(\delta_{ij}+\gamma\right) - b_srV_i^2\sin\gamma \tag{11}$$

$$Q_{\text{conv2}} = -b_srV_iV_j\cos\left(\delta_{ij}+\gamma\right) + b_srV_i^2\cos\gamma + b_sr^2V_i^2 \tag{12}$$

At last, the overall model of UPFC can be obtained by combining both shunt and series voltage source converter models as shown below. The overall UPFC model is depicted in Fig. 4.

$$\begin{aligned} P_i^{\text{UPFC}} &= b_srV_i^2\sin\gamma - b_srV_iV_j\sin\left(\delta_{ij}+\gamma\right) \\ P_j^{\text{UPFC}} &= b_srV_iV_j\sin\left(\delta_{ij}+\gamma\right) \end{aligned} \tag{13}$$

$$\begin{aligned} Q_i^{\text{UPFC}} &= -b_srV_i^2\cos\gamma \\ Q_j^{\text{UPFC}} &= b_srV_iV_j\cos\left(\delta_{ij}+\gamma\right) \end{aligned} \tag{14}$$

3 Optimization methods

3.1 Multiobjective cuckoo search algorithm

Cuckoo search (CS) algorithm was initially presented by Xin-She Yang and Suash Deb, inspired by the interesting breeding strategy of some cuckoo species (Yang and Deb 2009). Guria and Ani species of cuckoo family exhibit a peculiar behaviour concerning procreation. They identify a nest of any ill-fated host bird to dump their eggs. Such a breeding strategy alleviates the cuckoos from egg hatching, nurturing chicks, and protecting them from potential predators.

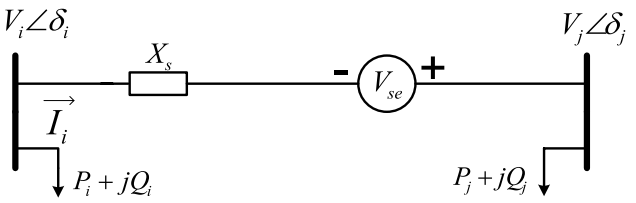

Fig. 4 Overall model of UPFC

The CS algorithm makes use of levy flights for its global search. Steps of a Levy flight are defined by step-lengths having probability distribution (Yang and Deb 2009). Levy flight is credited to be the optimal strategy for pursuing a target in an unknown environment as the probability of visiting the previously visited site is low. Levy flights application to optimization problems resulted in positive outcomes (Yang and Deb 2011).

The standard version of the CS algorithm consists of the following rules.

- Each cuckoo dumps one egg in any arbitrarily chosen nest
- The nests having best quality eggs will be made available for the next generations
- The number of available host nests being fixed, any fortunate host bird may identify the cuckoo eggs with a probability $p_a \in (0, 1)$. In such a situation, the host bird either abandons the nest or discards the eggs.

The modified first and last rules for the MOCS algorithm with n objectives are:

- Every cuckoo dumps n eggs in an arbitrarily chosen nest
- Fortunate host bird abandons each nest with probability p_a and a fresh nest will be created with n eggs based on the similarities/differences of the eggs. Random mixing can be employed to create diversity.

For every cuckoo i, a fresh solution $x^{(k+1)}$ can be produced from the old one $x^{(k+1)}$ by levy flight

$$x_i^{(k+1)} = x^{(k)} + \alpha \oplus Lévy(\lambda) \tag{15}$$

where α is the step size which is related to the scales of the specific problem, $\oplus$ is the Hadamard product operator. To provide room for the diversity in the quality of solution,α is produced as per the following equation.

$$\alpha = \alpha_0\left(x_j^{(k)} - x_i^{(k)}\right) \tag{16}$$

where α_o is a constant and $\left(x_j^{(k)} - x_i^{(k)}\right)$ is the difference of two arbitrary solutions which is adopted to represent the fact that similar eggs are less probable to detection by the host bird. Hence new solutions are produced by the proportionality of their difference. The step size, s, is defined as

$$S = \alpha_0\left(x_j^{(k)} - x_i^{(k)}\right) \oplus Lévy(\lambda) \sim 0.01\frac{U}{|V|^{1/\lambda}}\left(x_j^{(k)} - x_i^{(k)}\right) \tag{17}$$

where U and V are obtained from normal distributions. That is

$$U \sim N\left(0, \sigma_U^2\right), V \sim N\left(0, \sigma_V^2\right) \tag{18}$$

with

$$\sigma_U = \left\{\frac{\Gamma(1+\lambda)\sin(\pi\lambda/2)}{\lambda\Gamma\left[(1+\lambda)/2\right]2^{(\lambda-1)/2}}\right\}^{1/\lambda}, \sigma_V = 1, \tag{19}$$

where Γ is the standard Gamma function.

3.2 Multiobjective PSO:

Particle swarm optimization algorithm is introduced first by Kennedy and Eberhart (1995). PSO algorithm draws its inspiration from food foraging patterns of fish and bird swarms. The merits of PSO over its peers include reduced parameter requirements and shorter computation time. PSO algorithm consists of particles that are represented by their position and velocity. The location of a particle in search space is governed based on its own experience and from experience gained by its neighbor particles. Position and velocity are updated according to the following equations.

$$V_i(k+1) = w \times V_i(k) + c1 \times r1 \times \left(p\text{best}_i(k) - X_i(k)\right) + c2 \times r2 \times \left(g\text{best}(k) - X_i\right) \tag{20}$$

$$X_i(k+1) = X_i(k) + V_i(k+1) \tag{21}$$

where X_i is the position of the ith particle and velocity of the ith particle is V_i. k represents the current iteration, k+1 represents the next iteration values of the algorithm. $p\text{best}_i$ is the best particle value of ith particle and $g$best is the global best value among all particles. The overall flowchart for the optimization algorithms used is shown in Fig. 5.

4 Fitness function for minimization of losses

In general, an optimization problem with multi objectives comprises of multiple functions as a set of control variables that are to be minimized or maximized without violating the constraint limits.

$$\text{Minize } f_j(X, \sigma) = 0, j = 1, 2, \ldots\ldots..k_{\text{obj}} \tag{22}$$

Such that, $g(X, \sigma) = 0$ and $h(X, \sigma) = 0$.

where f_j is the j^{th} fitness function, k_{obj} is the number of fitness functions, $g(X, \sigma)$ is the equality constraints of the function and $h(X, \sigma)$ is inequality constraints of the function.

4.1 Formulation of objective functions

This study considers the following minimization functions for the estimation of power loss.

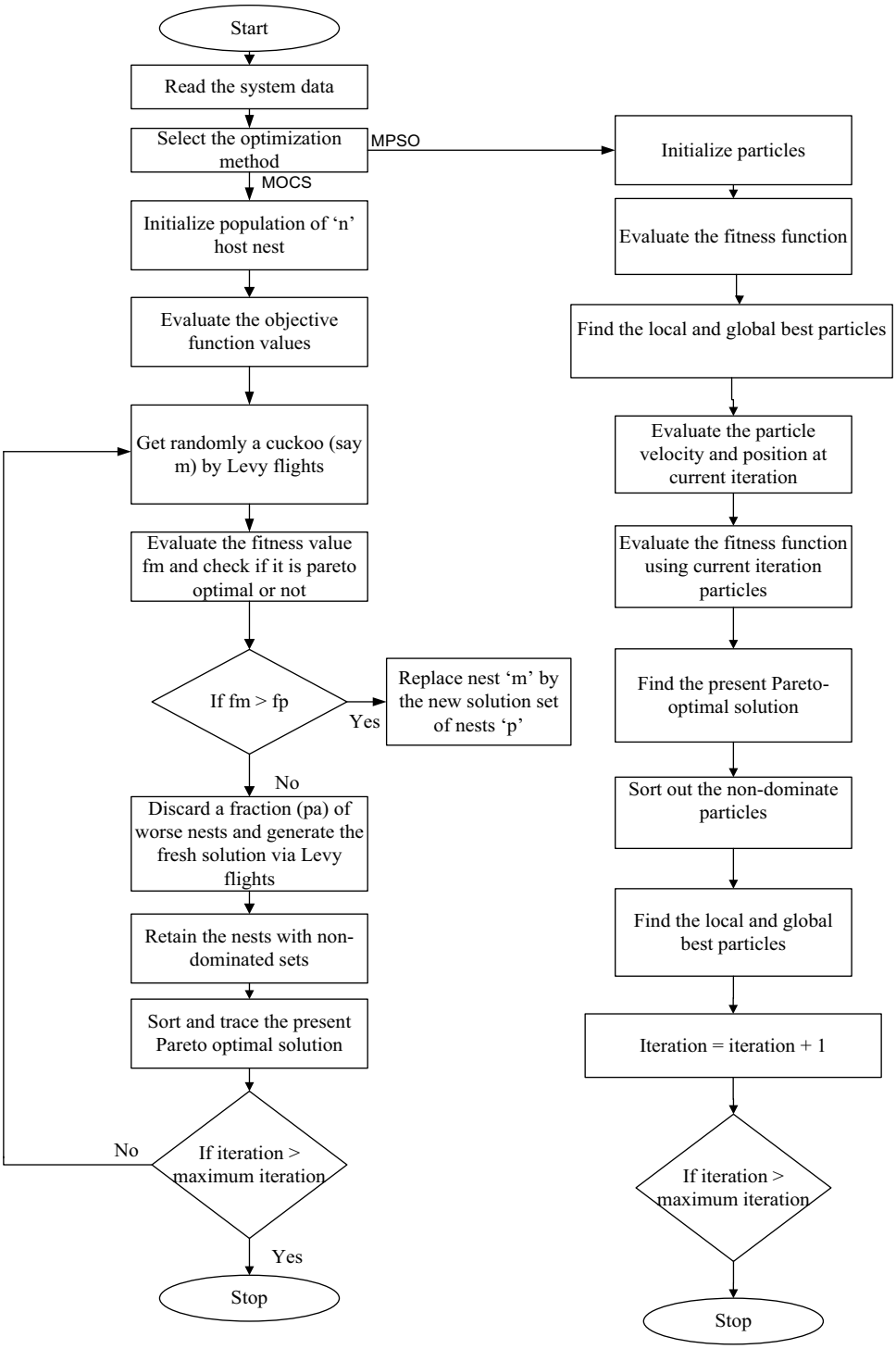

Fig. 5 Flowchart of MOCS and MOPSO algorithm

$$\mathrm{Min}(P_{\mathrm{Loss}}) = \sum_{m=1}^{NL} P_m \tag{23}$$

$$\mathrm{Min}\left(Q_{\mathrm{Loss}}\right) = \sum_{m=1}^{NL} Q_m \tag{24}$$

where NL is the number of lines, P_m is the active power loss in the line m, Q_m is the reactive power loss in the same line m

$$P_m = \left(V_i^2 + V_j^2 - 2V_iV_j\cos\delta_{ij}\right)\left(G_{ij}\right) \tag{25}$$

$$Q_m = \left(V_i^2 + V_j^2 - 2V_iV_j\cos\delta_{ij}\right)\left(B_{ij}\right) \tag{26}$$

Where,

V_i is the voltage magnitude at bus-i.

V_j is the voltage magnitude at bus-j.

G_{ij} is the conductance of the line admittance between bus-i and bus-j.

B_{ij} is the susceptance of the line admittance between bus-j and bus-j.

δ_{ij} is the phase shift between bus-i and bus-j respectively.

The variable constraints are given as follows:

(a) a. Equality constraints

$$P_{gi} - P_{di} = V_i \sum_{j=1}^{Nb} V_j\left(G_{ij}\cos\delta_{ij} + B_{ij}\sin\delta_{ij}\right) \tag{27}$$

$$Q_{gi} - Q_{di} = V_i \sum_{j=1}^{Nb} V_j\left(G_{ij}\mathrm{sn}\delta_{ij} - B_{ij}\cos\delta_{ij}\right) \tag{28}$$

where Nb is the number of buses, P_{gi} and Q_{gi} are the real and reactive power generation at bus-i, P_{di} and Q_{di} are the real and reactive power demand at bus-i.

(b) Inequality constraints

$$V_{Li}^{\min} \le V_{Li} \le V_{Li}^{\max} \tag{29}$$

$$V_{Gi}^{\min} \le V_{Gi} \le V_{Gi}^{\max} \tag{30}$$

$$Q_{Gi}^{\min} \le Q_{Gi} \le Q_{Gi}^{\max} \tag{31}$$

$$Q_c^{\min} \le Q_c \le Q_c^{\max} \tag{32}$$

$$T_s^{\min} \le T_s \le T_s^{\max} \tag{33}$$

$$V_{um}^{\min} \le V_{um} \le V_{um}^{\max} \tag{34}$$

$$\gamma_{um}^{\min} \le \gamma_{um} \le \gamma_{um}^{\max} \tag{35}$$

Where:

V_{Li} is the value of voltage at i^{th} load bus.

V_{Gi} is the value of voltage at i^{th} generator bus.

Q_{Gi} is the reactive power generation at i^{th} generator bus.

Q_c is the shunt capacitor reactive power generation at i^{th} bus.

T_s is the transformer tap setting ratio.

V_{um} is the voltage magnitude of UPFC at line-m, γ_{um} is the angle of UPFC at line-m.

5 Solution of the multiobjective problem

5.1 Pareto-optimal method

To solve the multiobjective optimization problem the Pareto-optimal method is exploited here in this work to produce a set of solutions. This method has the concept of dominance as its underlying principle. Vector V1 keeps dominating vector V2 given the below conditions are satisfied.

$$\forall k = \{1, 2, \ldots \ldots p\}, f_k(V1) \le f_k(V2) \tag{36}$$

$$\exists l \in \{1, 2, \ldots .p\} f_l(V1) < f_l(V2) \tag{37}$$

where p denotes the number of control variables.

5.2 Best-compromise solution

The best-compromise solution from the given set of Pareto-optimal solution is decided by the fuzzy logic method (Solmaz et al.2015). For this sake, a fuzzy membership function is devised for every objective function which is given as follows.

$$\mu_k(x) = \begin{cases} f_k^{\max} - f_k(x) & if\ f_k^{\min} < f_k < f_k^{\max} \\ 1, & if \quad f_k < f_k^{\min} \\ 0, & if \quad f_k < f_k^{\max} \end{cases} \tag{38}$$

where f_k^{min} and f_k^{max} corresponds to a totally permissible value and clearly impermissible value respectively, for the kth objective function. The membership function is given as follows.

$$\mu^r = \frac{\sum_{k=1}^{NO} \mu_k^r}{\sum_{k=1}^{ND}\sum_{k=1}^{NO} \mu_k^r} \tag{39}$$

where, for the rth non-dominated solution, *NO and ND* and are the number of objective functions and the number of Pareto-optimal solutions respectively. The solution that yields maximum membership is the best compromise solution.

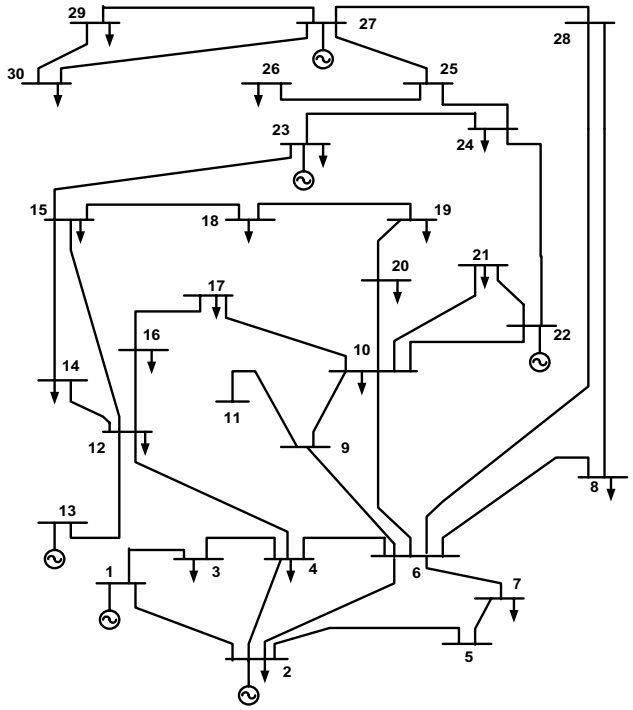

Fig. 6 Standard IEEE 30 bus system

6 Simulation results

To test the efficacy of the proposed MOCS algorithm for solving the multiobjective optimization problem under consideration, simulation is carried out in MATLAB on a standard IEEE 30 bus whose structure is shown in Fig. 6. The power losses are first calculated by MOCS algorithm without installing UPFC. Later, MOCS applied is applied to estimate power losses by installing UPFC a strategic position to show the effectiveness of UPFC in the reduction of power loss.

6.1 Power losses reduction without UPFC

Initially, a regular system without installing UPFC is considered and losses are computed. The share of active power loss is found to be 5.5933 MW, and the share of reactive power loss is 21.0658 MVar. Now to the test system is subjected to MOCS, MOPSO and MOFA techniques to compute the power loss. Table 1 presents the Pareto-optimal solution obtained after the application of MOCS, MOPSO and MOFA. The fuzzy logic method is employed to select the best-compromise solution from the pool of Pareto-optimal solution. The best-compromise solution generated by MOPSO for active power loss is 5.3046 MW and for reactive power loss is 20.4657 MVar while it is 5.2831 MW and 20.4437 MVar by MOCS for active power loss and reactive power loss respectively. The best-compromise solution obtained by MOFA for active power loss is 5.292 MW and for reactive power loss is 20.4561 MVar. It is evident from the results that the three algorithms are quite effective in the reduction of system power loss. The best-compromise solution obtained from MOFA is better that of MOPSO. It can also be noted that MOCS outperforms both MOPSO and MOFA as the obtained best-compromise solution for power loss reduction from MOCS is better than that of MOPSO and MOFA. Figure 7 comparatively depicts the results obtained from MOCS, MOPSO and MOFA algorithms.

The individual CPU time taken to run all the algorithms is shown in Table 2. It is observed that MOPSO is taking relatively less time when compared to MOCS and MOFA. Although MOCS gave a better result, its run time is relatively high.

6.2 Power losses reduction with UPFC:

In this study, the line losses are calculated after installing UPFC. For tracing the optimal position of UPFC installation, the total system losses are estimated by fitting UPFC at all the lines of the test system considering one line at a time. Table 3 shows the total losses with UPFC placement. It is evident from Table 3 that the lowest magnitude of the system losses is 5.2754 MW and 20.0162 MVar which is found at position 27–30. Hence the optimal position to install UPFC is the line connecting buses 27 and 30. The optimized parameters of UPFC are for the Eq. (13) and Eq. (14) are $r = 0.006$ and $\gamma = 90^0$. The parameters are tuned by considering the range mentioned in (Noroozian et al. 1997).

Now the test system is subjected to MOCS, MOPSO and MOFA techniques to compute the power loss by fixing UPFC at the optimal position, i.e., at 27–30. Table 4 shows the Pareto-optimal solution obtained after the application of MOCS, MOPSO and MOFA. The fuzzy logic method is employed to extract the best-compromise solution from the pool of Pareto-optimal solution. The best-compromise solution generated by MOPSO for active power loss is 5.0631 MW and for reactive power loss is 19.8832 MVar while it is 5.0375 MW and 19.8762 MVar by MOCS for active power loss and reactive power loss respectively. The best-compromise solution generated by MOFA for active power loss is 5.0406 MW and for reactive power loss is 19.8783 MVar It is evident from the results that UPFC placement resulted in a reduction of system power loss. It can also be noted that MOCS outperforms both MOFA and

Table 1 Comparison of Pareto-optimal solution without UPFC

	MOCS		MOPSO		MOFA	
Pareto optimal solutions	Active power losses(MW)	Reactive power losses(MVar)	Active power losses(MW)	Reactive power losses(MVar)	Active power losses(MW)	Reactive power losses(MVar)
1	5.2764	20.5992	5.2871	20.6231	5.2849	20.6076
2	5.2764	20.5958	5.2874	20.6223	5.2849	20.6024
3	5.2766	20.5926	5.2878	20.6165	5.2851	20.5971
4	5.2767	20.5893	5.2880	20.6106	5.2852	20.5918
5	5.2768	20.5861	5.2882	20.6049	5.2853	20.5862
6	5.2769	20.5804	5.2886	20.5991	5.2854	20.5811
7	5.2771	20.5747	5.2893	20.5932	5.2856	20.5759
8	5.2774	20.5691	5.2901	20.5876	5.2856	20.5707
9	5.2774	20.5634	5.2906	20.5819	5.2859	20.5654
10	5.2776	20.5574	5.2913	20.5760	5.2861	20.5603
11	5.2779	20.5516	5.2919	20.5702	5.2863	20.5551
12	5.2782	20.5457	5.2924	20.5645	5.2865	20.5499
13	5.2785	20.5396	5.2931	20.5587	5.2867	20.5448
14	5.2789	20.5388	5.2937	20.5528	5.2869	20.5396
15	5.2790	20.5279	5.2943	20.5471	5.2872	20.5343
16	5.2793	20.5221	5.2951	20.5413	5.2875	20.5292
17	5.2796	20.5162	5.2958	20.5357	5.2878	20.5239
18	5.2798	20.5104	5.2964	20.5299	5.2879	20.5187
19	5.2801	20.5046	5.2971	20.5240	5.2882	20.5134
20	5.2804	20.4987	5.2978	20.5183	5.2885	20.5083
21	5.2807	20.4930	5.2985	20.5124	5.2887	20.5031
22	5.2810	20.4872	5.2992	20.5066	5.2890	20.4978
23	5.2813	20.4816	5.2998	20.5010	5.2893	20.4927
24	5.2817	20.4757	5.3006	20.4952	5.2895	20.4874
25	5.2820	20.4698	5.3013	20.4894	5.2898	20.4822
26	5.2822	20.4643	5.3019	20.4837	5.2901	20.4769
27	5.2825	20.4586	5.3031	20.4780	5.2904	20.4717
28	5.2827	20.4526	5.3034	20.4721	5.2907	20.4666
29	5.2828	20.4472	5.3041	20.4692	5.2909	20.4613
30	**5.2831**	**20.4437**	**5.3046**	**20.4657**	**5.2912**	**20.4561**
31	5.2839	20.4434	5.3052	20.4655	5.2918	20.4558
32	5.2846	20.4431	5.3054	20.4653	5.2923	20.4556
33	5.2854	20.4431	5.3056	20.4652	5.2927	20.4556
34	5.2863	20.4431	5.3058	20.4650	5.2931	20.4553
35	5.2868	20.4428	5.3062	20.4650	5.2936	20.4553
36	5.2871	20.4428	5.3065	20.4649	5.2941	20.4552
37	5.2876	20.4428	5.3067	20.4649	5.2944	20.4552
38	5.2879	20.4428	5.3069	20.4649	5.2950	20.4552
39	5.2885	20.4428	5.3076	20.4649	5.2954	20.4552
40	5.2891	20.4428	5.3081	20.4649	5.2960	20.4552

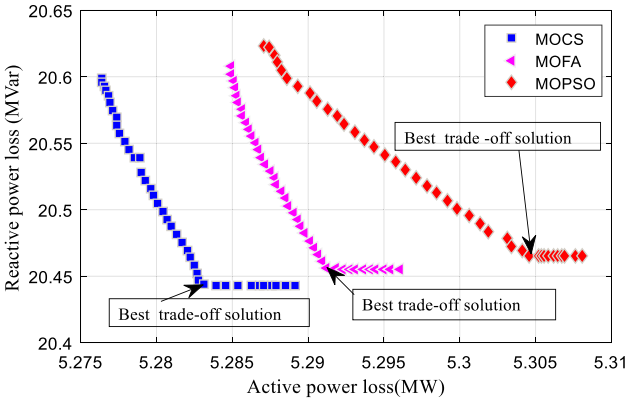

Fig. 7 Comparison of the best-compromise solution without UPFC

Table 2 CPU time without UPFC

Optimization method	CPU time in seconds
MOCS	96.991889
MOPSO	24.729699
MOFA	46.944513

MOPSO as the obtained best-compromise solution for power loss reduction from MOCS is better than that of MOFA and MOPSO. Figure 8 comparatively depicts the results obtained from MOCS, MOPSO and MOFA algorithms.

The individual CPU time taken to run all the algorithms after installation of UPFC at the optimal location is shown in Table 5. It is observed that MOPSO is taking relatively less time when compared to MOCS and MOFA. Although MOCS gave a better result, its run time is relatively high. It is also evident that the run time of all the algorithms increased after installing the UPFC.

A summary of all the results is shown in Table 6. It can be noted that before the installation of UPFC the power loss can be brought down by optimization. After the installation of UPFC, the power losses are further reduced. In both cases, MOCS has shown its superiority over MOPSO.

Table 3 Total losses with UPFC placement

Line number	From bus—To bus	Total power loss		Line number	From bus—To bus	Total power loss	
		P_{Loss} (MW)	Q_{Loss} (MVar)			P_{Loss} (MW)	Q_{Loss} (MVar)
1	1–2	5.3932	20.8703	22	15–18	5.5770	21.0185
2	1–3	5.5450	20.9846	23	18–19	5.5753	21.0186
3	2–4	5.5644	21.0296	24	19–20	5.5724	21.0137
4	3–4	5.5491	21.0924	25	10–20	5.5851	21.0379
5	2–5	5.4472	21.1006	26	10–17	5.5821	21.0165
6	2–6	5.5312	20.9557	27	10–21	5.5937	21.0751
7	4–6	5.5234	21.0189	28	10–22	5.5954	21.0584
8	5–7	5.4946	21.0873	29	21–22	5.5204	20.8655
9	6–7	5.5068	21.6947	30	15–23	5.5689	20.9946
10	6–8	5.5598	20.9837	31	22–24	5.5642	21.0030
11	6–9	5.5962	21.0500	32	23–24	5.5674	21.0018
12	6–10	5.5968	21.0554	33	24–25	5.5791	21.0023
13	9–11	5.5918	20.9762	34	25–26	5.5524	20.9718
14	9–10	5.5909	21.0253	35	25–27	5.5704	20.9758
15	4–12	5.5673	20.9147	36	28–27	5.5713	20.9672
16	12–13	5.5634	20.9277	37	27–29	5.3229	20.1004
17	12–14	5.5660	20.9640	38	**27–30**	**5.2754**	**20.0162**
18	12–15	5.5651	20.9901	39	29–30	5.2779	20.0184
19	12–16	5.5810	21.0042	40	8–28	5.5735	20.9949
20	14–15	5.5736	20.9819	41	6–28	5.5892	21.0500
21	16–17	5.5818	21.0173				

Table 4 Comparison of Pareto-optimal solution with UPFC

	MOCS		MOPSO		MOFA	
Pareto optimal solutions	Active power losses(MW)	Reactive power losses(MVar)	Active power losses(MW)	Reactive power losses(MVar)	Active power losses(MW)	Reactive power losses(MVar)
1	5.0312	20.0186	5.0395	20.0297	5.0349	20.0403
2	5.0313	20.0095	5.0398	20.0188	5.0351	20.0333
3	5.0314	19.9983	5.0406	20.0178	5.0352	20.0263
4	5.0316	19.9953	5.0414	20.0175	5.0354	20.0203
5	5.0317	19.9870	5.0421	20.0071	5.0355	20.0143
6	5.0318	19.9839	5.0429	20.0069	5.0357	20.0093
7	5.0320	19.9813	5.0435	20.0068	5.0359	20.0043
8	5.0321	19.9791	5.0437	19.9978	5.0362	19.9993
9	5.0324	19.9761	5.0445	19.9973	5.0364	19.9933
10	5.0327	19.9733	5.0453	19.9867	5.0365	19.9863
11	5.0330	19.9668	5.0460	19.9791	5.0368	19.9803
12	5.0333	19.9636	5.0468	19.9739	5.0370	19.9753
13	5.0336	19.9593	5.0476	19.9736	5.0372	19.9703
14	5.0338	19.9554	5.0484	19.9679	5.0375	19.9643
15	5.0342	19.9518	5.0492	19.9629	5.0376	19.9583
16	5.0346	19.9483	5.0500	19.9581	5.0378	19.9533
17	5.0347	19.9449	5.0507	19.9560	5.0381	19.9473
18	5.0349	19.9416	5.0518	19.9530	5.0383	19.9416
19	5.0351	19.9363	5.0525	19.9480	5.0386	19.9353
20	5.0355	19.9304	5.0533	19.9430	5.0387	19.9283
21	5.0359	19.9236	5.0541	19.9380	5.0389	19.9233
22	5.0364	19.9168	5.0549	19.9302	5.0392	19.9183
23	5.0367	19.9089	5.0557	19.9281	5.0395	19.9123
24	5.0369	19.8912	5.0565	19.9230	5.0392	19.9063
25	5.0372	19.8784	5.0573	19.9180	5.0394	19.9003
26	**5.0375**	**19.8762**	5.0581	19.9131	5.0396	19.8943
27	5.0379	19.8762	5.0592	19.9123	5.0398	19.8893
28	5.0381	19.8762	5.0601	19.9107	5.0401	19.8762
29	5.0386	19.8762	5.0613	19.9082	5.0403	19.8833
30	5.0392	19.8762	5.0619	19.9031	**5.0406**	**19.8783**
31	5.0397	19.8762	5.0622	19.8981	5.0411	19.8780
32	5.0403	19.8761	5.0625	19.8931	5.0415	19.8780
33	5.0412	19.8761	5.0627	19.8882	5.0420	19.8780
34	5.0421	19.8760	**5.0631**	**19.8832**	5.0425	19.8778
35	5.0429	19.8760	5.0636	19.8828	5.0429	19.8778
36	5.0436	19.8760	5.0638	19.8828	5.0432	19.8778
37	5.0441	19.8760	5.0641	19.8826	5.0436	19.8776
38	5.0447	19.8759	5.0645	19.8826	5.0441	19.8776
39	5.0452	19.8759	5.0647	19.8826	5.0445	19.8776
40	5.0458	19.8759	5.0648	19.8826	5.0449	19.8776

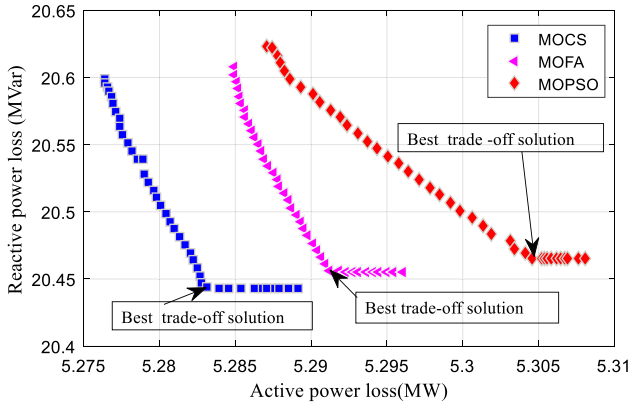

Fig. 8 Comparison of best-compromise solution with UPFC

Table 5 CPU time with UPFC

Optimization method	CPU time in seconds
MOCS	99.620892
MOPSO	26.037716
MOFA	51.959498

7 Conclusion and future scope

In this study, a multiobjective problem is presented to simultaneously reduce active and reactive power loss by fitting UPFC at a strategic position. MOCS a very popular and effective multiobjective algorithm is incorporated for this purpose. To ascertain the merit of UPFC installation in power loss reduction, the multiobjective function is optimized with and without installation of UPFC. Simulation results show that the optimal placement of UPFC can minimize the power losses. Reduction of power losses will enhance the system capacity without augmenting the generation capacity. Furthermore, the multiobjective problem considered is solved using MOPSO. Obtained results indicate that the MOCS algorithm is relatively more effective in optimizing the considered multiobjective problem. In this study, the methodology is verified on a standard IEEE 30 bus test system but the authors are of the opinion that the methodology may also be tested on various other standard test systems as an extension of this study. Furthermore, the robustness of the MOCS algorithm against various standard indices may also be checked. Also, various other FACTS devices like SVC, TCSC may be incorporated to reduce the power losses and comparison can be made among these devices to identify the better one.

Table 6 Summary of results with and without UPFC

Without UPFC								With UPFC					
Without optimization		MOCS		MOPSO		MOFA		MOCS		MOPSO		MOFA	
Active Power Loss (MW)	Reactive power loss (MVar)	Active Power Loss (MW)	Reactive power loss (MVar)	Active Power Loss (MW)	Reactive power loss (MVar)	Active Power Loss (MW)	Reactive power loss (MVar)	Active Power Loss (MW)	Reactive power loss (MVar)	Active Power Loss (MW)	Reactive power loss (MVar)	Active Power Loss (MW)	Reactive power loss (MVar)
5.593	21.0658	5.2831	20.4437	5.3046	20.4657	5.2912	20.4561	5.0375	19.8762	5.0631	19.8832	5.0406	19.8783

References

Dash SP, Subhashini KR, Satapathy JK (2019) Optimal location and parametric settings of FACTS devices based on JAYA blended moth flame optimization for transmission loss minimization in power systems. Microsyst Technol. https://doi.org/10.1007/s00542-019-04692-w

Dutta S, Roy PK, Nandi D (2015) Optimal location of UPFC controller in transmission network using hybrid chemical reaction optimization algorithm. Int J Electr Power Energy Syst 64:194–211

Galiana FD, Almeida K, Toussaint M, Griffin J (1996) Assessment and control of the impact of FACTS devices on power system performance. IEEE Trans Power Syst 11(4):1931–1936

Gyugyi L, Schauder CD, Williams SL, Rietman TR, Torgerson DR, Edris A (1995) The unified power flow controller: a new approach to power transmission control. IEEE Trans Power Deliver 10(2):1085–1097

Hingorani NG, Gyugyi L (2000) Understanding FACTS: concepts and technology of flexible AC transmission Systems. IEEE Press, New York

Kennedy J, Eberhart R (1995) Particle swarm optimization. In: IEEE International Conference on Neural Networks, Perth, pp. 1942–1948.

Mani SM, Seksena SBL (2017) A cost effective voltage sag compensator for distribution system. Int J Syst Assur Eng Manag 8(1):56–64

Mathur RM, Varma RK (2002) Thyristor-based FACTS controllers for electrical transmission systems. IEEE Press, New York

Nartu TR, Matta MS, Koratana S, Bodda RK (2019) A fuzzified Pareto multiobjective cuckoo search algorithm for power losses minimization incorporating SVC. Soft Comput 23:10811–10820

Noroozian M, Andersson G (1993) Power flow control by use of controllable series components. IEEE Trans Power Deliver 8(3):1420–1429

Noroozian M, Angquist L, Ghandhari M, Andersson G (1997) Use of UPFC for optimal power flow control. IEEE T Power Deliver 12(4):1629–1634

Mithu S (2013) Load flow studies with power injection model. Dissertation, National Institute of Technology, Rourkela, India.

Shaheen HI, Rashed GI, Cheng SJ (2008) Optimal location and parameters setting of UPFC based on GA and PSO for enhancing power system security under single contingencies. In: Proceedings of the IEEE Power and Energy Society General Meeting-Conversion and Delivery of Electrical Energy, Pittsburgh, pp. 1–8

Shrawane Kapse SS, Daigavane MB, Daigavane PM (2018) Improvement of ORPD Algorithm for Transmission Loss Minimization and Voltage Control Using UPFC by HGAPSO Approach. J Inst Eng India Ser B 99:575–585

Singh SN, Erlich I (2005) Locating UPFC for enhancing power system load-ability. In: 2005 International Conference on Future Power Systems. IEEE, pp. 1–5.

Solmaz K, Amin MH, Hazlie Bin M (2015) Comparative study of multi-objective optimal power flow based on particle swarm, evolutionary programming, and genetic algorithm. Electr Eng 97(1):1–1

Taher SA, Amooshahi MhK (2012) New approach for optimal UPFC placement using hybrid immune algorithm in electric power systems. Int J Electr Power Energy Syst 43:899–909

Venkatesh B, Gooi HB (2006) Optimal siting of unified power flow controller. Electr Power Compon Syst 34(3):46–69

Vijay BK, Ramaiah V (2019) Enhancement of dynamic stability by optimal location and capacity of UPFC: a hybrid approach. Energy. https://doi.org/10.1016/j.energy.2019.116464

Yang XS, Deb S (2009) Cuckoo search via l´evy flights. In: IEEE world congress on nature and biologically inspired computing, Coimbatore, India, pp 210–214

Yang XS, Deb S (2010) Engineering optimization by cuckoo search. Int J Math Model Numer Optim 1(4):330–343

Yang XS, Deb S (2011) Multiobjective cuckoo search for design optimization. Comput Oper Res 40(6):1616–1624